Available online at www.sciencedirect.com
SCIENCE DIRECT®
Journal of Chromatography A, 1058 (2004) 51–59
JOURNAL OF CHROMATOGRAPHY A
www.elsevier.com/locate/chroma

Fourier transform ion cyclotron resonance mass spectrometry of principal components in oilsands naphthenic acids

Mark P. Barrow[a,*], John V. Headley[b,**], Kerry M. Peru[b], Peter J. Derrick[a]

[a] *Institute of Mass Spectrometry and Department of Chemistry, University of Warwick, Coventry CV4 7AL, UK*
[b] *Aquatic Ecosystem Protection Research Branch, National Water Research Institute, 11 Innovation Boulevard, Saskatoon, Sask., S7N 3H5 Canada*

Abstract

Naphthenic acids present formidable challenges for the petroleum industry and are a growing concern in the aquatic environment. For example, these acids are responsible for corrosion of refinery equipment, leading to the incurrence of additional costs to the consumer, and are toxic to aquatic wildlife, making disposal and remediation of contaminated waters and sediments a significant problem. The detection and characterization of naphthenic acids is therefore of considerable importance. Fourier transform ion cyclotron resonance mass spectrometry is presented as a technique with inherently ultra-high mass accuracy and resolution, affording unequivocal assignments. The suitability of the technique for environmental applications is demonstrated to characterize two different commercial mixtures of naphthenic acids and one oilsands tailings pond sample.

Keywords: Naphthenic acids; Fourier transform ion cyclotron resonance; Mass spectrometry; Oilsands; Accurate mass; Ultra-high resolution

1. Introduction

1.1. Naphthenic acids

There is a need to develop routine and rugged methods for the determination of oilsands naphthenic acids in natural waters and contaminated soils. Complex mixtures of naphthenic acids, in particular, are known to be pre-disposed to leaching into subsurface soils and groundwater and that this transport is mobilized by their high water solubility. Naphthenic acids have been defined as carboxylic acids, which includes one or more saturated ring structures, where five- and six-membered rings are most common, though the definition has become more loosely used to describe the range of organic acids found within crude oils. The molecular formulae for the acids may be described by $C_nH_{2n+z}O_2$ [1–5] where "*z*" is referred to as the "hydrogen deficiency" and is a negative, even integer and more than one isomer will exist for a given *z* homolog. The carboxylic acid group is usually bonded or attached to a side chain, rather than directly to the cycloaliphatic ring [1,2] and the molecular weights differ by 14 mass units (CH_2) between *n* series and by two mass units (H_2) between *z* series [6]. Naphthenic acids are known to be slightly weaker acids than low molecular weight carboxylic acids, such as acetic acid [7]. Some naphthenic acids can be solubilised to produce metal salts that have industrial applications [4,8–10].

Naphthenic acids in the environment are relatively poorly studied, primarily because of their complex nature and need for rugged methods for their determination in soils, water and oilsands tailings wastewater. Although, naphthenic acids were first reported as oilsands components during the late 1960s, environmental assessment of naphthenic acids has been hampered, until recently, by a dearth of published analytical methods [11,12]. As a group, they co-occur with a diverse range of petroleum hydrocarbons present in oilsands deposits.

The presence of naphthenic acids in crude oils is one of the greatest concerns of the oil refining industry. Naph-

* Corresponding author. Tel.: +44 24 76572882; fax: +44 24 76524112.
E-mail addresses: m.p.barrow@warwick.ac.uk (M.P. Barrow), john.headley@ec.gc.ca (J.V. Headley).
** Co-corresponding author. Tel.: +306 975 5746; fax: +306 975 5143.

0021-9673/$ – see front matter © 2004 Elsevier B.V. All rights reserved.
doi:10.1016/j.chroma.2004.08.082

thenic acid corrosion of refinery units is agreed to be of increasing significance to industry and it has been claimed that savings of several dollars per barrel could be made if the corrosivity of the acids could be defined properly [13]. The naphthenic acid content of crude oils is believed to be on the rise due to the increasing use of "opportunity crude oils" [14]. The use of opportunity crude oils results from the increasing demand for oil and the increasing scarcity of resources, forcing the industry to utilize oilfields of lower quality. Turnbull et al. have shown that the size and structure of naphthenic acids influence their corrosivity [13].

In addition to costs incurred through naphthenic acid related corrosion, waste disposal is problematic for the petroleum industry. Naphthenic acids are known to be toxic to aquatic wildlife [15–17]. Wong et al. have demonstrated the use of granular activated carbon (GAC) to filter water and dramatically increase the survival rate of fish [3]. Thus far, most research conducted has focused on the environmental fate, transport and degradation, isolation of specific toxic naphthenic acids and epidemiology [18,19]. In a recent investigation of several commercial naphthenic acid mixtures and those extracted from oilsands, significant differences amongst four commercial mixtures and between the extracts from various oilsands ores and tailings ponds were established [20]. The naphthenic acids' concentrations and composition were highly varied amongst commercial sources, oilsands ore and tailings pond sources [20].

A variety of mass spectrometric techniques have been used for the structural elucidation of the acids, including: gas chromatography mass spectrometry (GC–MS) [1,4,21] liquid chromatography mass spectrometry (LC–MS) [22] utilizing a variety of ionization techniques such as electron ionization (EI) [4] liquid secondary ion mass spectrometry (LSIMS) [3] fast atom bombardment (FAB) [2] chemical ionization (CI) [1,2,4,5] atmospheric pressure chemical ionization (APCI) [5] and, recently, electrospray ionization (ESI) [23–25]. One of the greatest difficulties posed when characterizing the naphthenic acids found in crude oils is that it is not possible to chromatographically separate the many naphthenic acids species prior to mass spectrometric analysis [1,3,21]. As a result, mass spectrometric analysis leads to complex spectra displaying signals arising from hundreds of different acidic components. Various separation methods have been evaluated for general use with complex hydrocarbon mixtures, such as solid phase extraction (SPE) [26,27] and liquid chromatography mass spectrometry [28]. Illustrated here is an application of Fourier transform ion cyclotron resonance mass spectrometry (FT-ICR MS) for the characterization of naphthenic acids. The combination of the ultra-high mass accuracy, ultra-high resolution, and selective observation of the deprotonated naphthenic acids is demonstrated to make negative-ion mode FT-ICR MS the technique of choice for the characterization of oilsands naphthenic acids.

1.2. Fourier transform ion cyclotron resonance mass spectrometry

In general, the utility of FT-ICR MS for environmental applications is not well developed. A brief overview of the key features that pertain to the characterization of naphthenic acids is therefore given below. Full details of the FT-ICR MS methodology are described elsewhere [29–35]. In brief, the ions in an FT-ICR MS orbit in the presence of a strong magnetic field and the "cyclotron frequencies" of ions are measured, where these frequencies are related to the mass-to-charge ratios of the ions, as shown in Eqs. (1a) and (1b):

$$\omega = \frac{qB}{m} \tag{1a}$$

$$f = \frac{qB}{2\pi m} \tag{1b}$$

where m is the mass of the ion (in kg), ω the cyclotron frequency in terms of radians per second (rad s^{-1}), and f the cyclotron frequency in terms of hertz (Hz). Thus, ions of lower m/z have higher cyclotron frequencies than ions of higher m/z.

FT-ICR MS are best known for their excellent mass accuracy and resolution. Mass accuracy (measured in ppm) is a measurement of how well the observed m/z correlates with the "true value" and is particularly important for complex mixtures, where many possible elemental compositions could be assigned to a nominal, integer m/z value. Many other types of modern commercial mass spectrometers cite a specification of having a mass accuracy of the order of tens of ppm over a specific mass range, whereas specifications for FT-ICR MS frequently cite a mass accuracy of 1 ppm or better (lower). Eq. (2) is the relationship for determining the mass accuracy of a result when comparing the observed m/z with the value believed to be "true," called here the theoretical m/z:

$$\text{Mass accuracy} = \frac{m_{\text{observed}} - m_{\text{theory}}}{m_{\text{theory}}} \times 1\,000\,000 \tag{2}$$

where m_{observed} is the m/z of the peak of interest in the mass spectrum obtained and m_{theory} the theoretical m/z that would have been expected for the species.

Resolution is extremely important for resolving closely spaced signals, such as in the cases of complex mixtures or multiply-charged ions (as generated by electrospray ionization, for instance). The ability to use instruments with ultra-high resolution can sometimes make the difference between identifying and not identifying a species of interest. Eq. (3) defines the resolution:

$$\text{Resolution} = \frac{m}{\Delta m} \tag{3}$$

where m is the m/z of the peak of interest and Δm the width, in terms of m/z, determined, using any one of the many methods of mass spectrometry. Resolution can be measured, using the "10% valley" definition, as most commonly applied when using magnetic-sector instruments, or by using the full width

at half maximum (FWHM) definition, which is typically used during the analysis of data acquired from time-of-flight (TOF) or FT-ICR MS.

Whilst the resolution of many commercial time-of-flight mass spectrometers may approach approximately 10,000 and many commercial magnetic-sector mass spectrometers may approach a resolution of 100,000, high field FT-ICR MS can reach resolutions of hundreds of thousands in "broadband mode" ("normal" experimental conditions) or even reach a resolution of a few million in "heterodyne mode" (where a very narrow *m*/*z* range is studied but under very high resolution conditions). User expertise, however, is required to ensure that the instrument is properly tuned, ion populations in the FT-ICR analyzer cell are controlled, and that "space-charge effects," [36–38] which decrease resolution and mass accuracy, are minimized. "Peak coalescence" is one form of space-charge effect, where, for instance, two ion packets of similar frequency may interact and eventually process together, resulting in only one signal being observed. Peak coalescence is less of a problem when using stronger magnetic fields, due to the increased separation between ion packets in terms of frequency; the use of such a high field instrument has afforded the ability for the first time to resolve $^{12}C_{58}{}^{13}C_2{}^{+}$ and $^{12}C_{59}{}^{14}N^{+}$ during laser desorption/ionization experiments, for instance [39].

2. Experimental

2.1. Instrumentation

Throughout the course of the experiments described here, a 9.4 T Bruker BioApex II (Bruker Daltonics, Billerica, MA, USA) FT-ICR MS was used [40]. The heart of the instrument was the Infinity Cell [41] which was cylindrical in geometry, rather than the traditional cubic, and consisted of six plates: two trapping plates, two detection plates, and two excitation plates. The instrument was operated in the negative-ion mode throughout. During the course of these experiments, a trapping potential (PV1 and PV2) of −1.5 V was maintained to constrain the ions' movement within the cell and detection was performed over a mass range of *m*/*z* 86–2000, with the excitation range being slightly wider (*m*/*z* 75–2200) to compensate for possible non-homogeneities at the edges of the RF chirp used for excitation.

Ions were retained within the hexapole ion trap for a period of 2 s (D1 = 2 s) prior to extraction. The duration of the extraction pulse, referred to as P2, was set to 2400 μs. The SideKick mechanism was employed to deflect ions off axis as they enter the cell (EV1 = 1.10 V, EV2 = 1.60 V (where EV values corresponded to ICR cell extraction plates), DEV2 = −4.13 V (ICR cell delta extraction plate 2). Dipolar excitation was used to excite the ions to a detectable cyclotron orbit prior to the detection stage. The duration for the excitation steps, P3, was set to 12 μs, the RF attenuation for the excitation, PL3, was set to 11.26, and the excitation step size, XBB, was maintained at a value of 200. Data acquisition in broadband mode occurs, using a 12-bit, 10 MHz digitizer. The instrument was controlled using a Silicon Graphics Indy workstation running XMASS 5.0.10 (Bruker Daltonics, Billerica, MA, USA) under IRIX. 5.3. Data files consisted of 512 K (524,288) data points. The raw data must then be converted from the time domain to the frequency domain via a fast Fourier transform.

2.2. Samples

Two different commercial mixtures of naphthenic acids ("Fluka," "Acros,") and one tailings pond sample, hereafter referred to as "Syncrude," were investigated. The Fluka and Acros samples were neat naphthenic acid mixtures, whereas the Syncrude sample was an oilsands tailings pond alkaline extract. The Fluka and Acros samples were prepared for nanospray analysis by preparing a solution, using the ratio of 0.1 mg of crude oil per 1 mL of a 1:1 solvent mixture of methanol and water, while it was experimentally determined that the Syncrude sample concentration should be an order of magnitude higher (1 mg/mL of solvent mixture). Ammonia solution (35 vol.% in water, as the stock solution) was added to the sample solutions as 1% of the total volume, to assist deprotonation of the naphthenic acid species. The resulting solutions could then be used for nanospray analysis.

2.3. Instrumental analysis

A schematic of the nanospray apparatus used for the characterization of the various naphthenic acid mixtures is shown in Fig. 1. The apparatus is based upon the existing electrospray ion source (Analytica of Branford, USA) where a metal-coated glass needle replaces the arrangement of a metal needle connected in series to a syringe pump. Sample solution (10–20 μL) was transferred to the glass needle, and the needle was secured within a mount. Nanospray needles produced by Proxeon Biosystems (formerly Protana, Odense, Denmark) and New Objective (Woburn, MA, USA) were used throughout. When New Objective needles were used, the needle was simply positioned and the spray process could be initiated by determining the suitable capillary potential. When Proxeon needles were used a gas line was connected to the mount to provide a propelling gas; nitrogen was used as the gas of choice and a pressure of 10 psi was typically used. Proxeon needles have sealed tips which need to be broken prior to initialization of the spray; using a microscope to view the process, the sealed needle tip is carefully broken on a protective end cap placed over the Pyrex capillary, allowing the initiation of the spray of the sample solution. Positive-ion mode mass spectra of naphthenic acids have been previously observed to be more complex than the negative-ion mode mass spectra, with approximately three times as many signals being present. Negative-ion mode was therefore chosen as the most suitable method. Regardless of the nanospray needles used, the potential at the inside end of the capillary was maintained

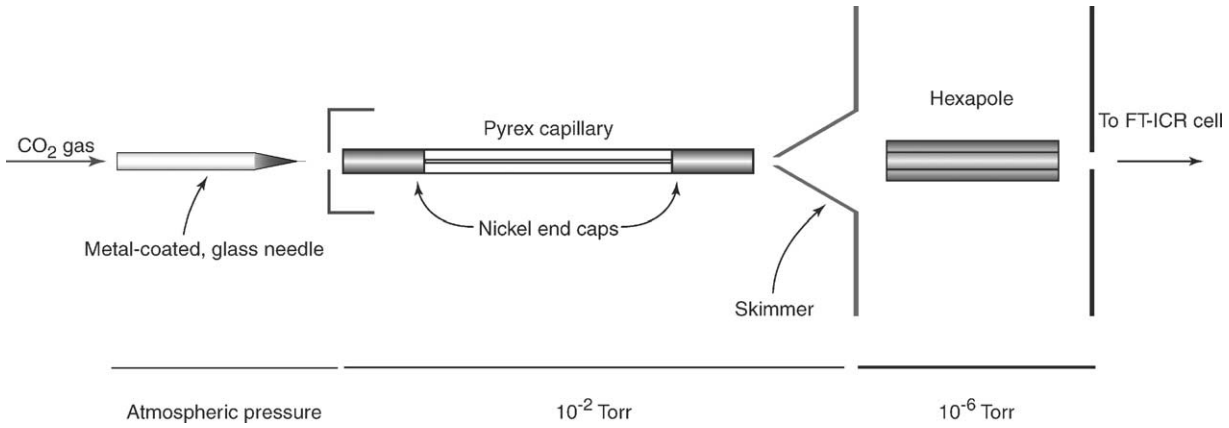

Fig. 1. Schematic diagram of the nanospray ion source. Ions are generated and transferred to the hexapole, where enough ions are accumulated prior to being pulsed into the FT-ICR cell for analysis.

at −110.40 V and the skimmer was set to −4.00 V. The potential difference between the nanospray needle and the outside end of the capillary was set to approximately 300 V when using Proxeon needles and approximately 600 V when using New Objective needles (which have a consistent tip diameter of 4 ± 1 μm, which is larger than that of the Proxeon needles, and therefore experience a weaker electrostatic field strength at the same potential). Some variation in capillary potential must be allowed for, due to the fact the needles will not be perfectly identical.

2.4. Data processing

Naphthenic acids have the molecular formula: $C_nH_{2n+z}O_2$, where z is a negative value and is frequently referred to as the "hydrogen deficiency." Once the mass spectra were obtained, the data were processed using XMASS. The Fluka and Acros samples were calibrated, using an electronic calibration reference list for naphthenic acids. The Syncrude sample was calibrated by exporting the calibration constants from the previously calibrated Acros mass spectrum. The relevant signals were sorted according to hydrogen deficiency, using a custom designed Microsoft Excel spreadsheet. The sorted data was then transferred to Microcal Origin for subsequent plots of the data. The results were displayed as plots of the relative intensities of the signals as a function of the carbon content (n), for the different hydrogen deficiencies. This effectively creates fingerprints for the different samples and can be used to trace the origins of the naphthenic acids.

3. Results and discussion

Previous work has included the successful application of negative-ion mode nanospray FT-ICR mass spectrometry for analysis of a range of crude oil extracts, to determine naphthenic acid species present [42]. Many mass spectrometric analyses of complex mixtures result in mass spectra with signals at nominal integer m/z values. The associated m/z assignments are also frequently quoted to one decimal place or sometimes to the integer value. Use of an instrument with a higher resolution and higher mass accuracy reveals information that is otherwise lost and, furthermore, the possibility that previous assignments based on m/z values to one decimal place or less could, in fact, be incorrect. "Doublets" can be observed [42], where species of a high hydrogen deficiency would simply have not been resolved at the resolution of conventional instrumentation, such as triple quadrupole mass spectrometers. The similarity in m/z also means that if only one decimal place (or less) is quoted, experimental error is sufficient to make the difference between a correct and an incorrect assignment of a molecular formula.

The Acros, Fluka, and Syncrude samples were analyzed in a similar manner to the crude oil extracts, using negative-ion mode nanospray ionization FT-ICR MS [42]. Fig. 2 shows the spectrum obtained for the Acros sample. The two most intense signals are found at m/z 213.185999 and m/z 297.279946, which are off-scale. Fig. 3a shows a smaller m/z

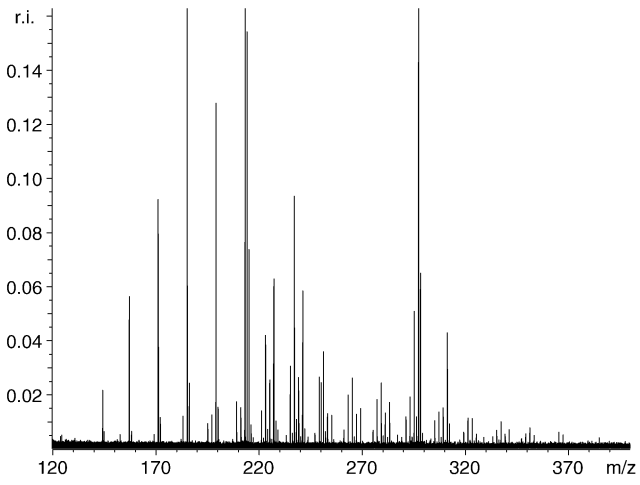

Fig. 2. Negative-ion mode broadband mass spectrum of the Acros sample, with the signals at m/z 213.185999 and m/z 297.279946 both off-scale.

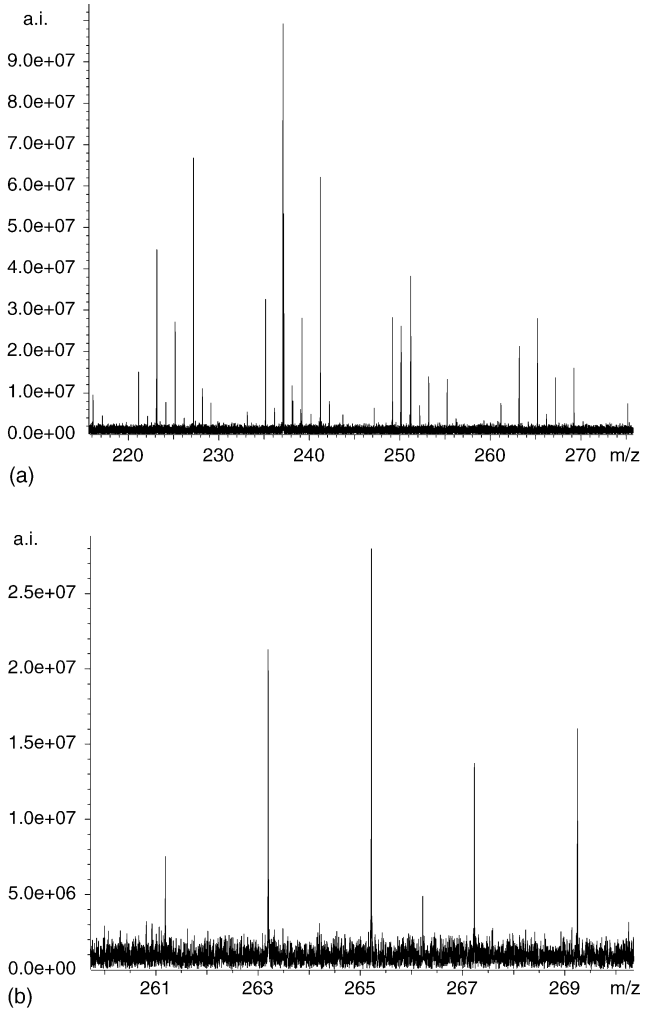

Fig. 3. (a) An enlarged region of Fig. 2, to enable the clearer observation of the less intense species. (b) A further enlarged *m*/*z* region, visible within Fig. 3(a) illustrating the number of signals present and the ability to differentiate between isotopomers (such as observed at approximately *m*/*z* 266).

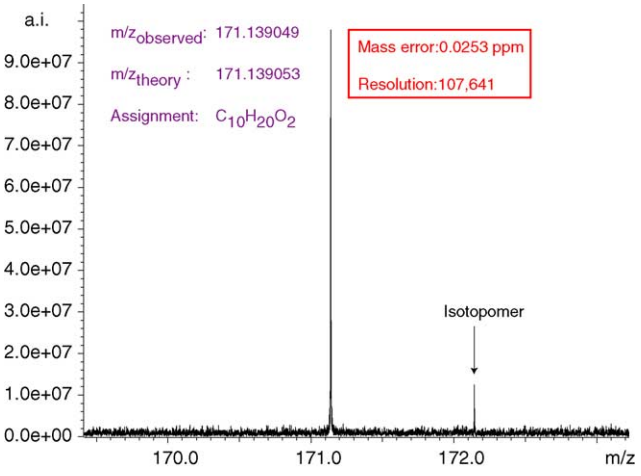

Fig. 4. An example of a single peak from a broadband negative-ion mode mass spectrum, obtained using a 9.4 T FT-ICR MS. In this particular case, the peak is taken from the mass spectrum of the Acros sample. The superior mass accuracy and resolution of the instrumentation are demonstrated.

range of Fig. 2, but the less intense species have been enlarged slightly to aid observation. Fig. 3b shows an enlarged *m*/*z* region of Fig. 3a, more clearly showing the presence of the isotopomers and illustrating the typical resolution that is obtained.

Fig. 4 highlights both the mass accuracy and the resolution associated with a Fourier transform ion cyclotron resonance mass spectrometer, which affords unequivocal assignment of molecular formulae. When considering mass accuracy, it is worth noting that the mass of an electron is approximately 0.5 mDa. The *m*/*z* discrepancy determined in Fig. 4 is therefore less than the mass of an electron, for example. Note that when calculating any theoretical *m*/*z*, whether manually or through the use of software, such as XMASS, the user must remember to take into consideration the gain or loss of elec-

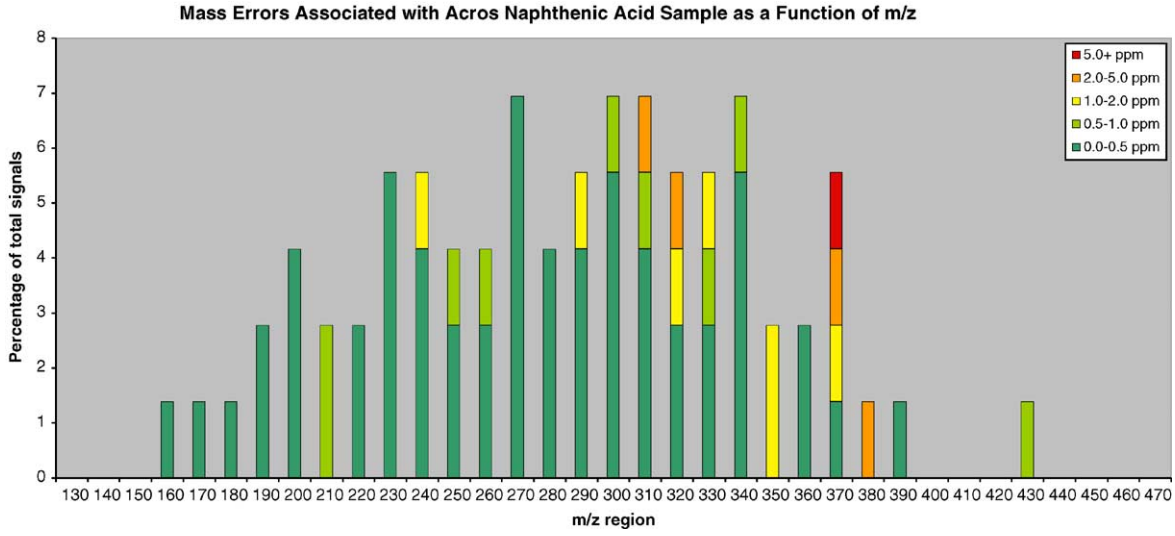

Fig. 5. The overall mass accuracies for the Acros sample.

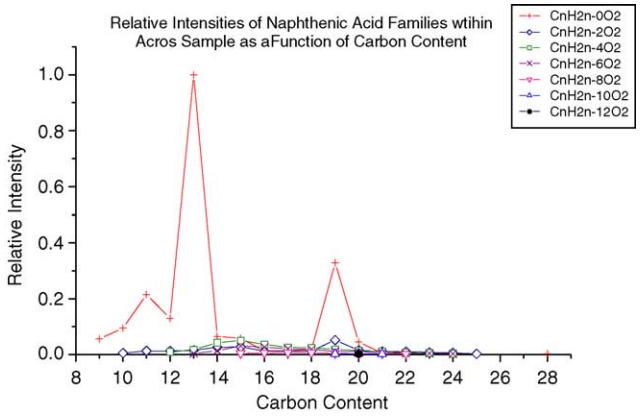

Fig. 6. Plot of relative intensity vs. carbon content for the different species within the Acros sample.

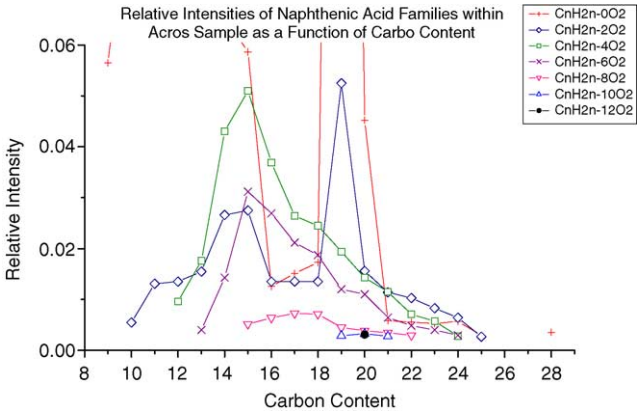

Fig. 7. Enlarged region of the plot of relative intensity vs. carbon content for the different species within the Acros sample, showing the less intense species more clearly.

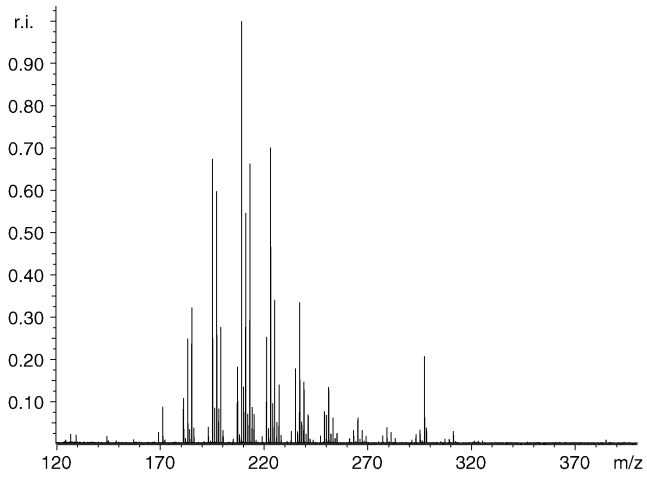

Fig. 8. Negative-ion mode broadband mass spectrum of the Fluka sample.

trons for the relevant charge state, for instance, by specifying the number of charges within XMASS.

Once all the signals had been "peak picked" (*m*/*z* labels given to the relevant signals manually), the data was exported as ASCII by using the ExportPeaks command within XMASS, and the pairs of *m*/*z* and relative intensity values were put into a custom designed Microsoft Excel spreadsheet for automated sorting. The spreadsheet automatically quotes the mass error associated with the experimental *m*/*z*. Over 77% of the signals had an associated mass accuracy within the 0.0–0.5 ppm range; the mass errors are displayed as a function of *m*/*z* in Fig. 5. The average relative mass error was calculated to be 0.57 ppm, with an associated standard deviation of 0.84. This is illustrative of the ultra-high mass accuracy associated with FT-ICR mass spectrometry, well

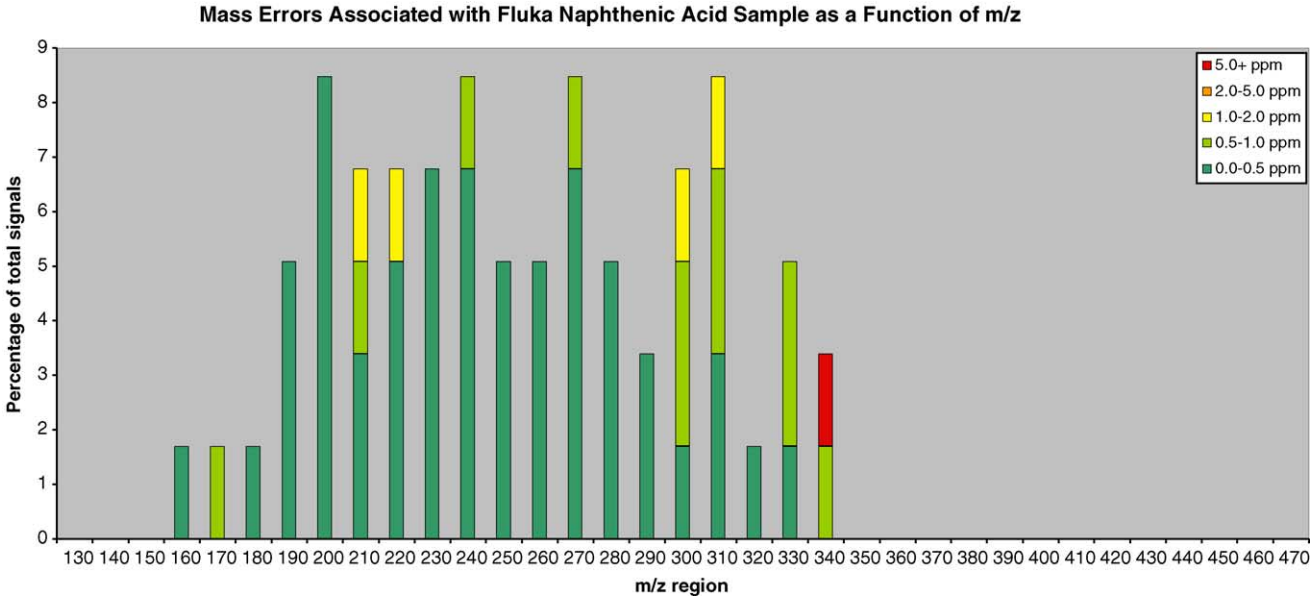

Fig. 9. The overall mass accuracies for the Fluka sample.

suited to the identification of individual components within complex naphthenic acid mixtures.

The sorted data was transferred to Microcal Origin for the purposes of plotting the relative intensities of the different species as a function of carbon content, as shown in Figs. 6 and 7. The most intense species observed were related to the $C_nH_{2n-0}O_2$ family, with the $C_nH_{2n-4}O_2$, $C_nH_{2n-2}O_2$, and $C_nH_{2n-6}O_2$ families being the next most intense. Lo et al. investigated the linear response of a mixture of naphthenic acids in the negative-ion mode and, despite the differences in structure, stated that the different naphthenic acid congeners do not interfere with one another in terms of the relative response [43]. In the current study, all instrument parameters were carefully controlled in order to ensure that the samples were studied under the same conditions. Thus, the plots for each sample (of the relative intensities of naphthenic acid species as a function of carbon content) could be compared in relative terms.

Fig. 8 shows the mass spectrum obtained for the Fluka sample, in which significant differences are evident for the Acros sample in terms of composition. The two signals that stand out most appear at *m/z* 209.154766 and *m/z* 297.279916. Once the signals had been peak picked, exported as ASCII, and sorted by Excel, the mass accuracies could be examined. Over 74% of the mass errors lay within the 0.0–0.5 ppm range. The mass errors are plotted as a function of *m/z* in Fig. 9, and the average relative mass error was determined to be 0.52 ppm, with an associated standard deviation of 0.96. The plot of relative intensities versus carbon content, shown in Fig. 10, revealed the most intense species were due to the $C_nH_{2n-4}O_2$, $C_nH_{2n-2}O_2$, and $C_nH_{2n-0}O_2$ families, which differed slightly from the Acros sample.

Fig. 11 shows a mass spectrum of the Syncrude sample. This sample represents a "real world" sample, whereas the

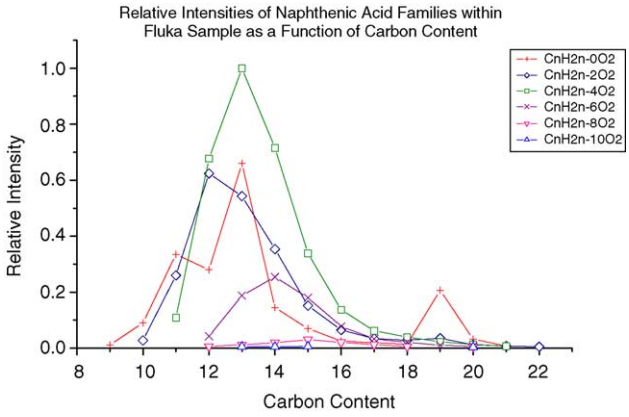

Fig. 10. Plot of relative intensity vs. carbon content for the different species within the Fluka sample.

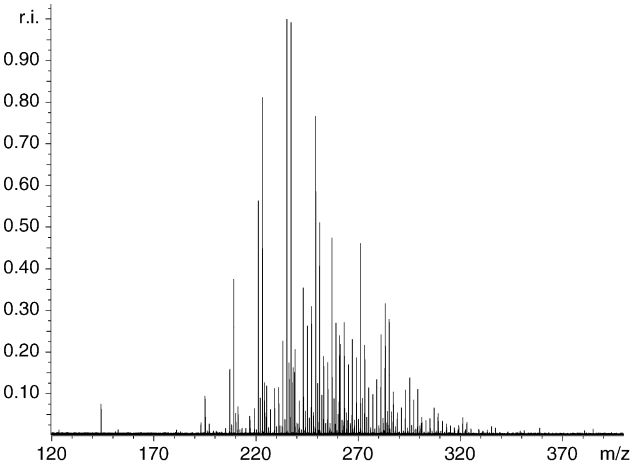

Fig. 11. Negative-ion mode broadband mass spectrum of the Syncrude sample.

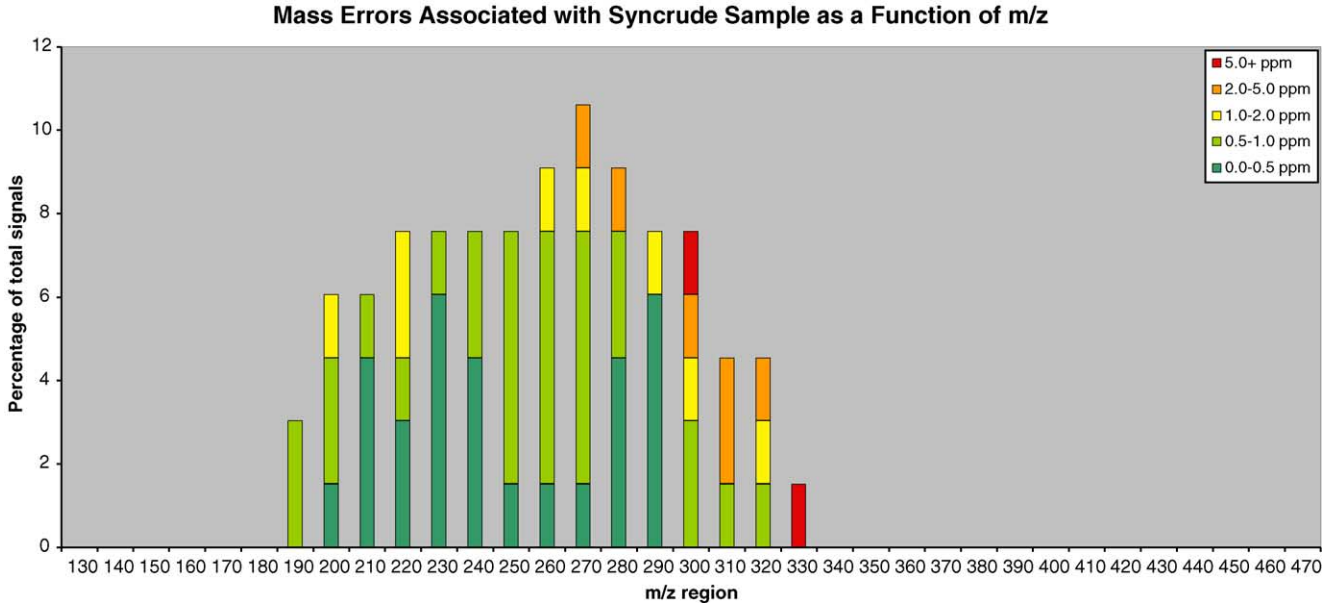

Fig. 12. The overall mass accuracies for the Syncrude sample.

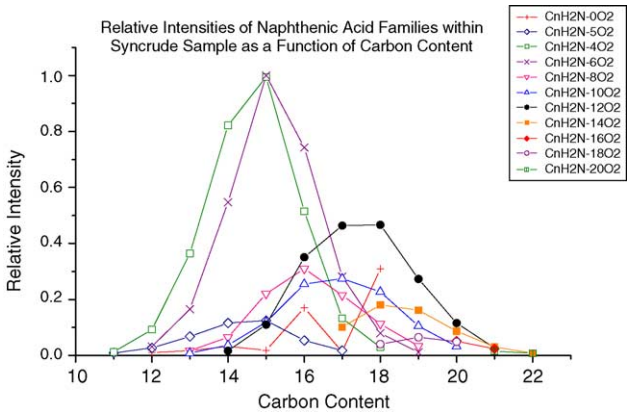

Fig. 13. Plot of relative intensity vs. carbon content for the different species within the Syncrude sample.

Acros and Fluka samples were commercial naphthenic acid samples. The mass spectrum for the Syncrude sample was comparatively more complex than the Acros and Fluka mass spectra. Fig. 11 was calibrated externally, using the calibration data from the Acros mass spectrum as the Acros data more closely correlated with the *m*/*z* range of interest than the Fluka data. The percentage of mass errors equal to or less than 0.5 ppm was lower than for the other samples (though over 76% was still better than 1 ppm), and this reflects the use of an external calibration. Fig. 12 shows a plot of the mass errors as a function of *m*/*z*, and the relative mass error was calculated to be 1.14 ppm, with a standard deviation of 1.27.

Fig. 13 shows the plot of the relative intensities for the different naphthenic acid species detected, as a function of carbon content. The $C_nH_{2n-4}O_2$ and $C_nH_{2n-6}O_2$ families were clearly the most intense, though the $C_nH_{2n-12}O_2$ family was also surprisingly intense, with a maximum being located at 18 carbon atoms. The plot illustrates the fact that more species were present in the sample, as was first indicated by the comparatively complex mass spectrum shown in Fig. 11.

The total percentage of signals with a mass accuracy of 1 ppm or better for the Acros, Fluka, and Syncrude samples were 87.32, 93.11, and 76.12%, respectively; it should be noted that the percentages were rounded to the nearest 0.01% within Microsoft Excel. Although, the mass accuracy associated with an externally calibrated spectrum is lower, it has nevertheless, been demonstrated that the mass accuracy remains extremely high and is relevant to the analysis of "real world" samples. FT-ICR MS using high magnetic fields are most noticeably set apart from other varieties of mass spectrometer by their inherently ultra-high mass accuracy and resolution, and therefore afford unequivocal assignments of species present within complex mixtures.

4. Conclusion

Fourier transform ion cyclotron resonance mass spectrometers utilizing high magnetic fields are inherently capable of ultra-high resolution and mass accuracy, which proves invaluable when analyzing complex mixtures such as naphthenic acid mixtures. FT-ICR mass spectrometry not only affords unequivocal assignments of signals, but also provides information that other instrumentation miss, such as the presence of naphthenic acids of a high hydrogen deficiency. The latter were evident for the complex mixtures of naphthenic acids investigated, illustrating the utility of FT-ICR mass spectrometry for the characterization of oilsands naphthenic acids.

Acknowledgements

Financial support was provided in part by the Panel of Energy Research and Development (PERD).

References

[1] I. Dzidic, A.C. Somerville, J.C. Raia, H.V. Hart, Anal. Chem. 60 (1988) 1318.
[2] T.-P. Fan, Energy Fuels 5 (1991) 371.
[3] D.C.L. Wong, R. van Compernolle, J.G. Nowlin, D.L. O'Neal, G.M. Johnson, Chemosphere 32 (1996) 1669.
[4] W.P. St. John, J. Rughani, S.A. Green, G.D. McGinnis, J. Chromatogr. A 807 (1998) 241.
[5] C.S. Hsu, G.J. Dechert, W.K. Robbins, E.K. Fukuda, Energy Fuels 14 (2000) 217.
[6] D.C. Herman, P.M. Fedorak, J.W. Costerton, Can. J. Microbiol. 39 (1993) 576.
[7] B.P. Tissot, D.H. Welte, Petroleum Formation and Occurrence, Springer-Verlag, Berlin, 1984.
[8] J.B. Davis, Petroleum Microbiology, Elsevier Publishing Company, Amsterdam, 1967.
[9] D.C. Herman, P.M. Fedorak, M.D. MacKinnon, J.W. Costerton, Can. J. Microbiol. 40 (1994) 467.
[10] J.A. Brient, Proceedings of the 215th National Meeting on Am. Chem. Soc., 1998, p. 131.
[11] W.K. Seifert, R.M. Teeter, W.G. Howells, M.J.R. Cantow, Anal. Chem. 41 (1969) 1638.
[12] L.R. Nascimento, L.M.C. Rebouças, L. Koike, F.D.M. Reis, A.L. Soldan, J.R. Cerqueira, et al., Org. Geochem. 30 (1999) 1175.
[13] A. Turnbull, E. Slavcheva, B. Shone, Corrosion 54 (1998) 922.
[14] E. Slavcheva, B. Shone, A. Turnbull, Br. Corros. J. 34 (1999) 125.
[15] M.D. MacKinnon, H. Boerger, Water Pollut. Res. J. Can. 21 (1986) 496.
[16] J.V. Headley, C. Akre, F.M. Conly, K.M. Peru, L.C. Dickson, Environ. Forensics 2 (2001) 335.
[17] F.M. Conly, J.V. Headley, R.W. Crosley, J. Environ. Eng. Sci. 1 (2002) 187.
[18] W.K. Seifert, R.M. Teeter, Anal. Chem. 42 (1970) 750.
[19] W.K. Robbins, Proceedings of the 215th National Meeting on Am. Chem. Soc., 1998, p. 137.
[20] J.S. Clemente, N.G.N. Prasad, M.D. MacKinnon, P.M. Fedorak, Chemosphere 50 (2003) 1265.
[21] J.B. Green, B.K. Stierwalt, J.S. Thomson, C.A. Treese, Anal. Chem. 57 (1985) 2207.
[22] C.S. Hsu, M.A. McLean, K. Qian, T. Aczel, S.C. Blum, W.N. Olmstead, et al., Energy Fuels 5 (1991) 395.
[23] K. Miyabayashi, K. Suzuki, T. Teranishi, Y. Naito, K. Tsujimoto, M. Miyake, Chem. Lett. (2000) 172.
[24] K. Miyabayashi, N. Yasuhide, M. Miyake, K. Tsujimoto, Eur. J. Mass Spectrom. 6 (2000) 251.

[25] D. Zhan, J.B. Fenn, Int. J. Mass Spectrom. 194 (2000) 197.
[26] B. Bennett, S.R. Larter, Anal. Chem. 72 (2000) 1039.
[27] D.M. Jones, J.S. Watson, W. Meredith, M. Chen, B. Bennett, Anal. Chem. 73 (2001) 703.
[28] K. Qian, C.S. Hsu, Anal. Chem. (1992) 2327.
[29] M.B. Comisarow, A.G. Marshall, Chem. Phys. Lett. 25 (1974) 282.
[30] M.B. Comisarow, A.G. Marshall, Can. J. Chem. 52 (1974) 1997.
[31] M.B. Comisarow, A.G. Marshall, Chem. Phys. Lett. 26 (1974) 489.
[32] C.B. Jacoby, C.L. Holliman, M.L. Gross, Fourier Transform Mass Spectrometry: Features, Principles, Capabilities and Limitations, Kluwer Academic Publishers, Netherlands, 1992.
[33] A.G. Marshall, L. Schweikhard, Int. J. Mass Spectrom. Ion Process. 118/119 (1992) 37.
[34] I.J. Amster, J. Mass Spectrom. 31 (1996) 1325.
[35] A.G. Marshall, C.L. Hendrickson, G.S. Jackson, Mass Spectrom. Rev. 17 (1998) 1.
[36] Y. Naito, M. Inoue, Int. J. Mass Spectrom. Ion Process. 157/158 (1996) 85.
[37] J.T. Stults, Anal. Chem. 69 (1997) 1815.
[38] J.E. Bruce, G.A. Anderson, H.R. Udseth, R.D. Smith, Anal. Chem. 70 (1998) 519.
[39] X. Feng, N. Clipston, T. Brown, H. Cooper, U. Reuther, A. Hirsch, et al., Rapid Commun. Mass Spectrom. 14 (2000) 368.
[40] M. Palmblad, K. Hakansson, P. Hakansson, X. Feng, H.J. Cooper, A.E. Giannakopulos, et al., Eur. J. Mass Spectrom. 6 (2000) 267.
[41] P. Caravatti, M. Allemann, Org. Mass Spectrom. 26 (1991) 514.
[42] M.P. Barrow, L.A. McDonnell, X. Feng, J. Walker, P.J. Derrick, Anal. Chem. 75 (2003) 860.
[43] C.C. Lo, B.G. Brownlee, N.J. Bunce, Anal. Chem. 75 (2003) 6394.